IMPROVED PERFORMANCE OF PASSIVE LAYER-FREE CURVED PMUT ARRAY

Chichen Huang[1], Shubham Khandare[2], Sri-Rajasekhar Kothapalli[2] and Srinivas Tadigadapa[1]
[1]Northeastern University, USA
[2] The Pennsylvania State University, USA

ABSTRACT

We have successfully demonstrated a novel, passive layer-free, curved piezoelectric micromachined ultrasound transducer (PMUT) array, using a sacrificial curved glass template and 30% scandium-doped aluminum nitride (Sc-AlN) as the active layer. The PMUTs were fabricated using a curved, suspended borosilicate glass template created via a chip-scale glass-blowing technique, onto which electrodes and the piezoelectric layer were deposited. The glass layer was thereafter selectively removed. We characterized the performance of a 13 × 13 curved PMUT (cPMUT) array using an electrical impedance analyzer, a Laser Doppler Vibrometer (LDV), and hydrophone pressure measurements. Our results reveal a device resonance frequency of approximately 1.8 MHz in air, with LDV analysis indicating a significantly enhanced low-frequency response of 1.68 nm/V—a fivefold improvement over conventional curved PMUTs with a passive layer. Additionally, acoustic characterization in water showed that this array generates an acoustic pressure of approximately 80 kPa at a 4.4 mm focal distance, with a beam width of 5 mm, and achieves a spatial peak pulse average intensity (ISPPA) of 216 mW/cm^2 when driven off-resonance. Furthermore, we demonstrate 20-degree steering capability using our data acquisition system. These advancements highlight significant potential for enhancing the precision and efficacy of medical imaging and therapeutic applications, particularly in ultrasonic diagnostics and treatments.

KEYWORDS

Ultrasound transducers array, scandium-doped aluminum nitride, chip-scale glass blowing, curved glass structures, piezoelectric micromachined ultrasound transducer (PMUT), curved PMUTs (cPMUT)

INTRODUCTION

Ultrasound technology is extensively utilized in the medical field, leveraging its unique capability to propagate through various tissues. This attribute is crucial for a range of biomedical applications. The non-invasive nature of ultrasound, combined with its ability to achieve sub-millimeter spatial resolution at depths of several centimeters, highlights its importance in contemporary medical practices. Notable applications include diagnostic imaging [1], therapeutic interventions such as tumor treatment using high-intensity focused ultrasound (HIFU)[2], ultrasound-guided drug delivery[3], and the treatment of neural disorders using low-intensity focused ultrasound (LIFU) via neuro-stimulation [4] and modulation[5].

Ultrasound transducers can be categorized into two main types: conventional bulk piezoelectric transducers and MEMS-based transducers, also referred to as micro-machined ultrasound transducers (MUTs). Both types have been effectively employed in neuromodulation applications [6], [7]. MUTs, which operate in plate flexural mode, provide several advantages over traditional thickness mode transducers, including compact size, cost-effective batch fabrication, lower costs, and enhanced flexibility in frequency ranges. These attributes make MUTs particularly suitable for implantable and wearable ultrasound devices.

The two primary variants of MUTs are piezoelectric micromachined ultrasonic transducers (PMUTs) and capacitive micromachined ultrasonic transducers (CMUTs), each offering unique benefits. CMUTs are known for their high electromechanical coupling factors, although they require high operational bias voltages, typically ranging from 10 to 100 V. In contrast, PMUTs operate at lower voltages and impedance, making them more energy efficient. However, PMUTs have lower electromechanical coupling factors, which results in diminished acoustic pressure outputs. These contrasting characteristics underscore the ongoing development and optimization of ultrasound transducer technology for diverse medical applications.

Research efforts have focused on enhancing the pressure outputs of PMUTs, primarily through modifications in diaphragm geometry and electrode design configurations, representing the most pursued approaches in this endeavor. For instance, the utilization of a two-port electrode design has yielded a doubled acoustic output when compared to unimorph planar PMUTs [8]. Furthermore, bimorph PMUTs, featuring two active AlN layers, achieved a fourfold increase in acoustic output compared to similarly sized unimorph PMUTs [9] at the cost of increased fabrication and operation complexity.

Curved PMUT has been studied recently both analytically [10] and experimentally [11], [12], promising advancements in their characteristics and pressure output. This progress is chiefly credited to their unique mechanical mechanism. Unlike planar PMUTs, where membrane movement is generated from the moment introduced by in-plane stress mismatch between piezoelectric and passive layers, curved PMUTs utilize the vertical component of in-plane stress in the same direction as the vibration. Consequently, the removal of the passive layer becomes a feasible approach to obtain a higher electro-mechanical coupling coefficient.

Different fabrication methods have been used in the previous research to realize curved PMUTs. A wax mold method was used to fabricate curved zinc oxide based PMUTs, but it had limitations in large-scale array fabrication [13]. Thin film PZT-based curved PMUTs [11] were reported to have an excellent electromechanical coupling factor of 45%, but they lack CMOS compatibility and biocompatibility. Recently, curved PMUTs have been fabricated via CMOS-compatible techniques, using wet isotropic etching of silicon followed by the deposition of low-temperature oxide (LTO) and aluminum nitride (AlN), but resulted in underutilized wafer areas and arrays with low fill-factors [14].

Lately, chip-scale glass blowing technique has surfaced as a promising approach for producing curved PMUTs [12], providing good control over membrane curvature for achieving different device sizes without the limitations associated with prior fabrication approaches. This technique also enables the fabrication of CMOS compatible and high fill-factor array with efficient utilization of wafer real estate. Recently, we reported the pressure measurement of a curved Sc-AlN PMUT array with a 5 μm passive layer [15].

In this study, we will present the fabrication and characterization of a 13 × 13 element, passive layer-free, curved PMUT array fabricated using the chip-scale glass blowing technique. The device was first characterized in air with LDV and impedance analysis, followed by hydrophone measurement of the pressure field.

FABRICATION

The specification of the fabricated PMUT array is shown in Table 1 and the four- mask fabrication flow is shown in Fig. 1. The silicon wafer was patterned with circle arrays using the first mask and was etched to a depth of 250 µm with silicon DRIE. Then, it was anodically bonded to a 100-µm-thick borosilicate glass (Schott Borofloat 33) wafer in vacuum (10^{-4} Torr). The wafer stack was then diced into smaller sub-wafer. The glass blowing was performed after thinning the glass using wet etching in HF. To control the curvature depth, the sub-wafer was heated to the glass transition temperature (525°C) and left for 30 minutes to stabilize. The curvature depth was then measured with a surface profilometer. This glass-blowing process was repeated with a 25°C increment until the desired depth was reached. Subsequently, bottom electrode stacks of 20 nm/100 nm Ti/Pt were deposited onto the curved glass template and patterned using the second mask. 750 nm thick layer of 30% Sc-AlN film was sputtered, followed by the deposition of the top electrode consisting of 20 nm/100 nm Cr/Au. The top electrode was then patterned using the third mask via an etching process, and the Sc-AlN layer was etched using RIE to create vias to the bottom electrode with the fourth mask. Thereafter, the sub-wafer was diced into 5 mm square chips. The backside of the Si was ground using a diamond grinding pad on an AutoMet 250 machine (Buehler, Lake Bluff, IL) until the etch holes were exposed. Subsequently, the chip was etched in HF with the front side protected to remove the glass template. Fig. 2 shows a microscope image of the backside of the chip after grinding (left) and the fabricated 13 × 13 curved PMUT array (right).

Table 1: Specification of PMUT in this work

Device Layer	Design Specifications		
	Diameter size (µm)	*Thickness (µm)*	*Depth of Curvature (µm)*
30% Sc-AlN	150	0.75	4~5.8
Ti/Pt Bottom Electrode		0.020/0.1	
Cr/Au Top Electrode		0.020/0.1	
Silicon Substrate		200	

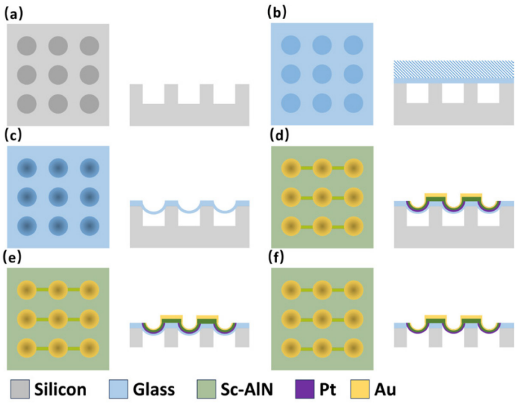

Figure 1: Process flow of proposed passive-layer-free curved PMUT array. (a) patterning Si substrate by DRIE, (b) anodic bonding and etching of glass, (c)glass blowing (d) depositing and patterning Pt/Sc-AlN/Au. (e) backside Si grinding, (f) backside glass etching.

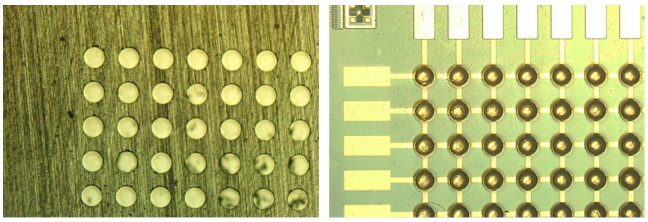

Figure 2: (left)Backside of the device after grinding; (right) front side of the device.

RESULTS AND DISCUSSION

Air-coupled Characterization

The PMUT array was initially measured using a Laser Doppler Vibrometer (LDV) to obtain its frequency response. Each PMUT cell had 31 scan points, and only the z-direction detector was enabled. During each measurement, three elements were connected and scanned. In the first experiments, the PMUT was excited by a wideband periodic chirp signal. Figure 3(a) illustrates the average displacement measured across the scan area, encompassing all cells, when driven by the chirp signal. The center frequency in air was determined to be approximately 1.8 MHz.

It's worth noting that LDV is limited to measuring velocity or displacement when the target is in motion. Therefore, low frequency off-resonance LDV measurements away from the resonance frequency of the device allow for estimation of the DC flexural (quasi-static) performance of the cells. In this study, the PMUT was driven by a 500 kHz sine signal to capture the low-frequency displacement. The displacement amplitude of the center point of each cell from element #3 to element #13 are plotted against the cell number.as illustrated in the Fig. 3(b). One of the elements was not working properly due to the bottom electrode damage and is considered as outlier. The average displacement was 1.68 nm/V with standard deviation of 0.41 nm/V. The typical Q-factor of these cells was 20 – 40. The displacement observed here is approximately five times higher than that reported for the curved PMUT with a passive layer in our previous work [12]. Furthermore, a lower Q factor is desirable for imaging applications, as it leads to a broader bandwidth, enhancing overall performance.

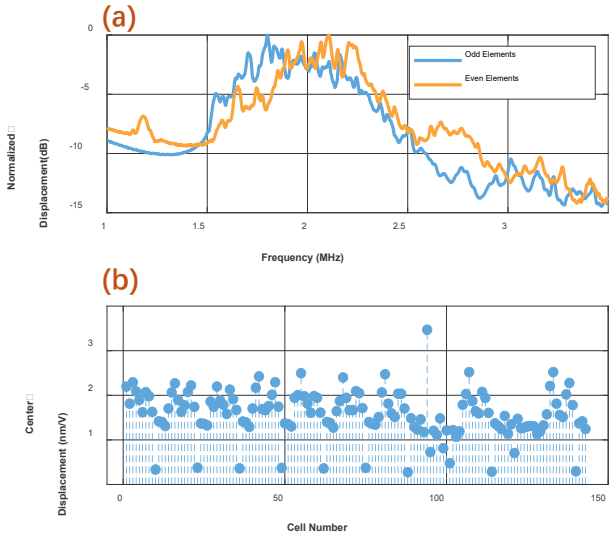

Figure 3: LDV measurements: (a)averaged displacements of all cells, (b)off-resonance displacements of each PMUT cell.

It's observed that there was nonuniformity across the chip. In Fig. 3(b), the displacement exhibited a discernible trend within each element, suggesting that along this direction, there was variation in curvature. Specifically, it appears that the curvature of cell #1 was shallower than that of cell #2. This observation aligns with the surface profilometer measurement, which indicated that the curvatures of the cells varied from 4 to 5.8 µm along the elements.

Fig. 4 is the impedance measurement in air for element #3 from the same device. which exhibited a resonance frequency of around 1.8 MHz. The electromechanical coupling coefficient is calculated as 2.5% in air from Fig. 4 using the resonance and anti-resonance frequencies equation.

$$k_t^2 = \frac{f_a^2 - f_r^2}{f_a^2} \quad (1)$$

where f_r is the resonant frequency and, f_a is the anti-resonant frequency.

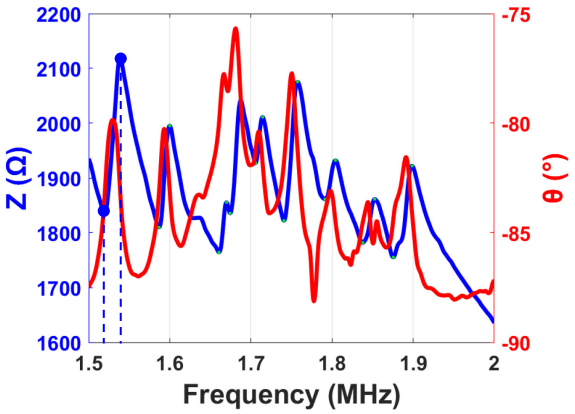

Figure 4: Impedance measurement of element#3

Hydrophone Characterization

After the air-coupled characterization, the PMUT array was coated with a layer of parylene-C polymer for the purpose of acoustic pressure characterization in water. The resonance frequency of the curved PMUT array was predicted using FEA simulation and the analytical equation for the planar PMUT [16],

$$f_{0,fluid} \approx \frac{f_{0,air}}{\sqrt{1+0.34\frac{\rho_{fluid} d}{\mu}}} \quad (2)$$

Where, $\mu = \sum_{i=1}^{n} \rho_i t_i$, ρ_i is density of layer in pMUT membrane, t_i thickness of the layer in pMUT membrane, ρ_{fluid} is density of the fluid, and d diameter of the membrane. Both methods predicted a resonance frequency of 500-800 kHz when immersed in water.

The Verasonics data acquisition system, in our laboratory can only drive at frequencies above 2 MHz, and therefore all pressure characterization reported here was performed at an off-resonance frequency which is significantly higher than the fundamental resonance frequency of the array. The experimental setup of the hydrophone measurements is shown in Fig. 5. The MATLAB-based programming interface of the Vantage 256 system (Verasonics, Inc, Kirkland, WA) is used to implement custom beamforming algorithms for optimized focusing of the 13 x 13 PMUT array. A capsule hydrophone (ONDA, HGL-080, Onda Corporation, Sunnyvale, CA) mounted on a 3D positioning system is used to map the acoustic pressure field generated by the PMUT array. The hydrophone is scanned across the acoustic field along a 2D XZ plane perpendicular to the PMUT array surface. At each location, the hydrophone captured both the pressure amplitude and phase details. This information is then used to construct a 2D representation of the acoustic pressure distribution produced by the PMUT array.

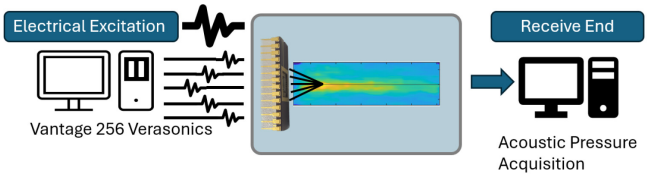

Figure 5: The schematic of acoustic pressure characterization using a hydrophone and the Vantage 256 ultrasound data acquisition system.

Fig. 6 shows the acoustic pressure map of the PMUT array steered at angles -10°, 0°, and +10°, respectively. The input excitation wave is programmed to transmit ultrasound pulses from the array in row-addressable mode using the Vantage 256 system at a 22 Vp-p. The performance of the array is tested under higher harmonic mode of vibration at an off-resonance frequency of 2 MHz of 2 cycles of a sine wave. The capsule hydrophone recorded acoustic pressure up to ~80 kPa at a focal zone ~ 4.4 *mm* away from the array with a beam width of 5 *mm*. The input signal is beamformed by controlling timing and apodization for the array elements of the PMUT array to generate steering angles of -10°, 0°, +10°. The spatial peak pulse average intensity, I_{SPPA}, is calculated to be around 216 mW/cm^2 demonstrates the suitability of the PMUT array for biomedical applications.

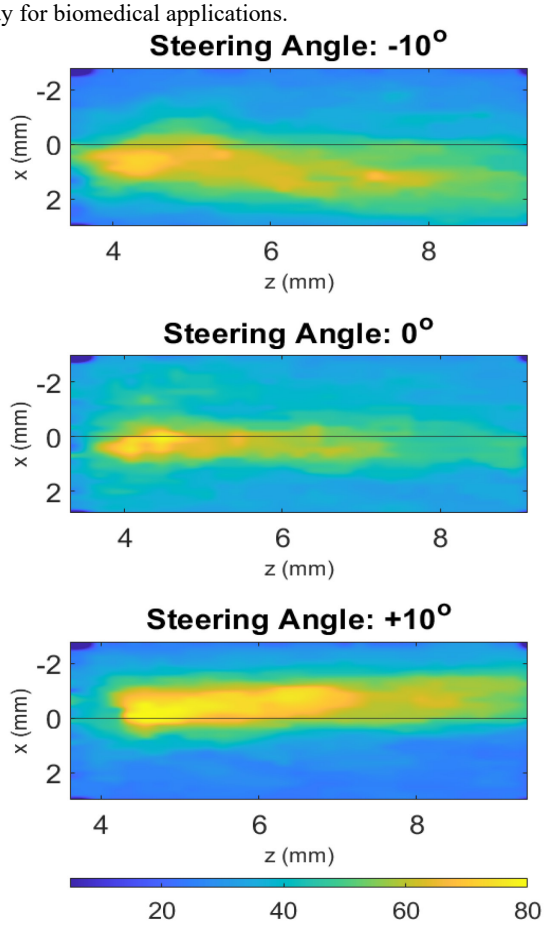

Figure 6: Acoustic pressure map (in kPa) in the XZ-plane of 13 × 13 element passive layer-free curved PMUT array driven at 22 V, 2 cycles, 2 MHz of sine wave, steer angle = -10°, 0°, +10°.

Table 2: Comparison of metrics of curved PMUT with and without passive layer.

Metrics	W/O Passive Layer (This Work)	W/ Passive Layer [12], [15]
Low-frequency Displacement (nm/V)	1.68	0.3
Quality Factor	20-30	100-150
Coupling Coefficient (k_t^2)	2.5%	2%
Pressure at 2MHz (kPa/V)	7.27*	8.49**
* Measured Off-Resonance; ** Measured at Resonance		

Table 2 compares the metrics of the curved PMUT with and without a passive layer, illustrating significant performance enhancements. It's important to note that the pressure in this work of the passive layer-free PMUTS was measured off-resonance, whereas the result for the curved PMUT with a passive layer was measured at its resonance and explains why the pressure output of the passive layer-free PMUT is lower than that with the passive layer. With the Q-factor of around 20, the at-resonance pressure is expected to be an order of magnitude larger and will be experimentally confirmed in future work.

CONCLUSION

We present the characterization of curved Piezoelectric Micromachined Ultrasound Transducers (PMUTs), notable for their unique design without a passive layer. These three-dimensional PMUTs were templated on curved suspended glass diaphragms, achieved using the chip-scale glass-blowing method, followed by the removal of the glass layer from the backside.

The performance of a 13 × 13 curved PMUT array was assessed using electrical impedance, Laser Doppler Vibrometry (LDV), and hydrophone measurements. The passive layer-free PMUT exhibited a much lower quality factor and improved off-resonance displacement compared to PMUTs with a passive layer, indicating a broader bandwidth for the device. The pressure map obtained at the off-resonance frequency also suggests a wide operable bandwidth.

ACKNOWLEDGEMENTS

This work was supported by the National Science Foundation (NSF) under Grant 2053591.

REFERENCES

[1] L. G. Montilla, R. Olafsson, D. R. Bauer, and R. S. Witte, "Real-time photoacoustic and ultrasound imaging: A simple solution for clinical ultrasound systems with linear arrays," *Phys Med Biol*, vol. 58, no. 1, Jan. 2013, doi: 10.1088/0031-9155/58/1/N1.

[2] R. O. Illing *et al.*, "The safety and feasibility of extracorporeal high-intensity focused ultrasound (HIFU) for the treatment of liver and kidney tumours in a Western population," *Br J Cancer*, vol. 93, no. 8, pp. 890–895, Oct. 2005, doi: 10.1038/sj.bjc.6602803.

[3] S. Mitragotri, "Healing sound: the use of ultrasound in drug delivery and other therapeutic applications," *Nat Rev Drug Discov*, vol. 4, no. 3, pp. 255–260, 2005, doi: 10.1038/nrd1662.

[4] E. Rezayat and I. G. Toostani, "A review on brain stimulation using low intensity focused ultrasound," *Basic and Clinical Neuroscience*, vol. 7, no. 3. Iran University of Medical Sciences, pp. 187–194, 2016. doi: 10.15412/J.BCN.03070303.

[5] H. S. Gougheri, A. Dangi, S. R. Kothapalli, and M. Kiani, "A Comprehensive Study of Ultrasound Transducer Characteristics in Microscopic Ultrasound Neuromodulation," *IEEE Trans Biomed Circuits Syst*, vol. 13, no. 5, pp. 835–847, Oct. 2019, doi: 10.1109/TBCAS.2019.2922027.

[6] C. Seok, O. J. Adelegan, A. O. Biliroglu, F. Y. Yamaner, and O. Oralkan, "A Wearable Ultrasonic Neurostimulator - Part II: A 2D CMUT Phased Array System with a Flip-Chip Bonded ASIC," *IEEE Trans Biomed Circuits Syst*, vol. 15, no. 4, pp. 705–718, Aug. 2021, doi: 10.1109/TBCAS.2021.3105064.

[7] H. Kim *et al.*, "Miniature ultrasound ring array transducers for transcranial ultrasound neuromodulation of freely-moving small animals," *Brain Stimul*, vol. 12, no. 2, pp. 251–255, Mar. 2019, doi: 10.1016/j.brs.2018.11.007.

[8] F. Sammoura, S. Shelton, S. Akhbari, D. Horsley, and L. Lin, "A two-port piezoelectric micromachined ultrasonic transducer," in *2014 Joint IEEE International Symposium on the Applications of Ferroelectric, International Workshop on Acoustic Transduction Materials and Devices & Workshop on Piezoresponse Force Microscopy*, 2014, pp. 1–4. doi: 10.1109/ISAF.2014.6923004.

[9] S. Akhbari, F. Sammoura, C. Yang, M. Mahmoud, N. Aqab, and L. Lin, "Bimorph pMUT with dual electrodes," in *Proceedings of the IEEE International Conference on Micro Electro Mechanical Systems (MEMS)*, Feb. 2015, pp. 928–931. doi: 10.1109/MEMSYS.2015.7051112.

[10] F. Sammoura, S. Akhbari, and L. Lin, "An analytical solution for curved piezoelectric micromachined ultrasonic transducers with spherically shaped diaphragms," *IEEE Trans Ultrason Ferroelectr Freq Control*, vol. 61, no. 9, pp. 1533–1544, 2014, doi: 10.1109/TUFFC.2014.3067.

[11] F. Calame and P. Muralt, "Novel 3D PZT thin film structure for micromechanics," *J Electroceram*, vol. 19, no. 4, pp. 399–402, Dec. 2007, doi: 10.1007/s10832-007-9054-1.

[12] C. Huang, S. P. Khandare, S. R. Kothapalli, and S. Tadigadapa, "Characterization of Curved Piezoelectric Micromachined Ultrasound Transducers Fabricated by Chip-Scale Glass Blowing Technique," *IEEE Sens Lett*, vol. 7, no. 10, Oct. 2023, doi: 10.1109/LSENS.2023.3308112.

[13] G. H. Feng, C. C. Sharp, Q. F. Zhou, W. Pang, E. S. Kim, and K. K. Shung, "Fabrication of MEMS ZnO dome-shaped-diaphragm transducers for high-frequency ultrasonic imaging," *Journal of Micromechanics and Microengineering*, vol. 15, no. 3, pp. 586–590, Mar. 2005, doi: 10.1088/0960-1317/15/3/021.

[14] S. Akhbari, F. Sammoura, S. Shelton, C. Yang, D. Horsley, and L. Lin, "Highly responsive curved aluminum nitride PMUT," in *Proceedings of the IEEE International Conference on Micro Electro Mechanical Systems (MEMS)*, 2014, pp. 124–127. doi: 10.1109/MEMSYS.2014.6765589.

[15] S. P. Khandare, C. Huang, S. R. Kothapalli, and S. Tadigadapa, "Performance of Aluminum Nitride Curved PMUT Arrays Fabricated Using Glass Blowing Technique," in *Proc. of the IEEE International Conference on Micro Electro Mechanical Systems (MEMS)*, 2024, pp. 198–201. doi:10.1109/MEMS58180.2024.10439406.

[16] X. Jiang *et al.*, "Monolithic ultrasound fingerprint sensor," *Microsyst Nanoeng*, vol. 3, 2017, doi: 10.1038/micronano.2017.59.